Journal of Organometallic Chemistry 962 (2022) 122272

Contents lists available at ScienceDirect

Journal of Organometallic Chemistry

journal homepage: www.elsevier.com/locate/jorganchem

Incorporation of metal-chelating unnatural amino acids into halotag for allylic deamination

Alina Stein [a,b], Alexandria Deliz Liang [a,b,c], Reyhan Sahin [a], Thomas R. Ward [a,b,*]

[a] Department of Chemistry, University of Basel, Mattenstrasse 24a, 4058 Basel, Switzerland
[b] National Center of Competence in Research, Molecular Systems Engineering, Basel, Switzerland
[c] Department of Chemistry, University of Zurich, Winterthurerstrasse 190, 8057 Zurich, Switzerland

ARTICLE INFO

Article history:
Received 2 December 2021
Revised 19 January 2022
Accepted 21 January 2022
Available online 23 January 2022

Keywords:
HaloTag
Unnatural amino acid
Deallylation
Artificial metalloenzyme
Metal-chelating

ABSTRACT

The potential of artificial metalloenzymes has led to an increase in interest for the design of novel metal-binding sites in proteins. Metal-chelating unnatural amino acids offer an auspicious solution to engineer active metal sites in a defined way. Herein, we describe the introduction of four metal-chelating unnatural amino acids into HaloTag, an attractive scaffold for the assembly of functional artificial metalloenzymes. HaloTag, engineered with 2-amino-3-(8-hydroxyquinolin-5-yl)propanoic acid (HQ-Ala-1) was used to assemble an artificial metalloenzyme for improved allylic deamination upon complementation with $[(\eta^5\text{-}C_5H_5)Ru(MeCN)_3]^+$.

1. Introduction

Artificial Metalloenzymes (ArMs) are versatile tools in bioengineering. They can be obtained by introducing an abiotic transition metal cofactor into a protein scaffold, thus leading to a merging of the reactivity of transition metals with the selectivity and specificity of enzymes [1–5]. Several scaffolds have been used to assemble ArMs. The most widely studied host proteins include: (strept)avidin [6–8], LmrR [9,10], myoglobin [11–17], human carbonic anhydrase II [18], cytochromes [19–24], azurin [25], prolyl oligopeptidase [26], nitrobindin [27,28], human serum albumin [29], designer scaffolds [30–34] etc. [1]. Recently, our group has used HaloTag as scaffold for the generation of an artificial metalloenzyme that catalyzes olefin metathesis [35]. HaloTag is a self-labeling protein that forms a covalent bond with linear haloalkanes to generate an ester. It is derived from a bacterial enzyme, Rhodococcus dehalogenase (DhaA) [36].

While the selection of an appropriate scaffold has drawn much attention, the plethora of available ArMs has also been expanded by the incorporation of unnatural amino acids (UAAs) [37]. The canonical DNA-encoded amino acids provide broad, yet limited functionalities. To date, more than 200 structurally different UAAs have been incorporated into proteins in E. coli [38], mammalian cells [39] and animals [40]. A few reported UAAs can chelate metal ions. Recent years have, therefore, witnessed the incorporation of metal-chelating UAAs into protein hosts to genetically incorporate metal binding sites [30,41–55]. In this work, we set out to capitalize on the HaloTag (version 7) for the assembly of an artificial deallylase resulting from the incorporation of a metal-chelating UAA and subsequent incubation with $[(\eta^5\text{-}C_5H_5)Ru(MeCN)_3]^+$ to afford a hybrid catalyst for the deallylation of carbamates (Fig. 1) [56–59]. Such a system offers several attractive features including: i) the metal binding site can be introduced (nearly) anywhere within the protein, ii) the metal binding site is genetically encoded, thus simplifying the assembly of an ArM with a well-localized and defined metal site, and iii) it is possible to create enzymes bearing more than one active site [60].

2. Materials and methods

2.1. Reagents and chemicals

For the synthesis of 2-amino-3-(8-hydroxyquinolin-5-yl)propanoic acid and 2-amino-3-[4–*hydroxy*-3-(1H-*pyrazol*-1-*yl*)*phenyl*]propanoic acid and for information on commercially available reagents and chemicals please refer to the supplementary information.

Abbreviations: ArM, Artificial Metalloenzyme; UAA, Unnatural Amino Acid.

* Corresponding author.
E-mail address: thomas.ward@unibas.ch (T.R. Ward).

https://doi.org/10.1016/j.jorganchem.2022.122272

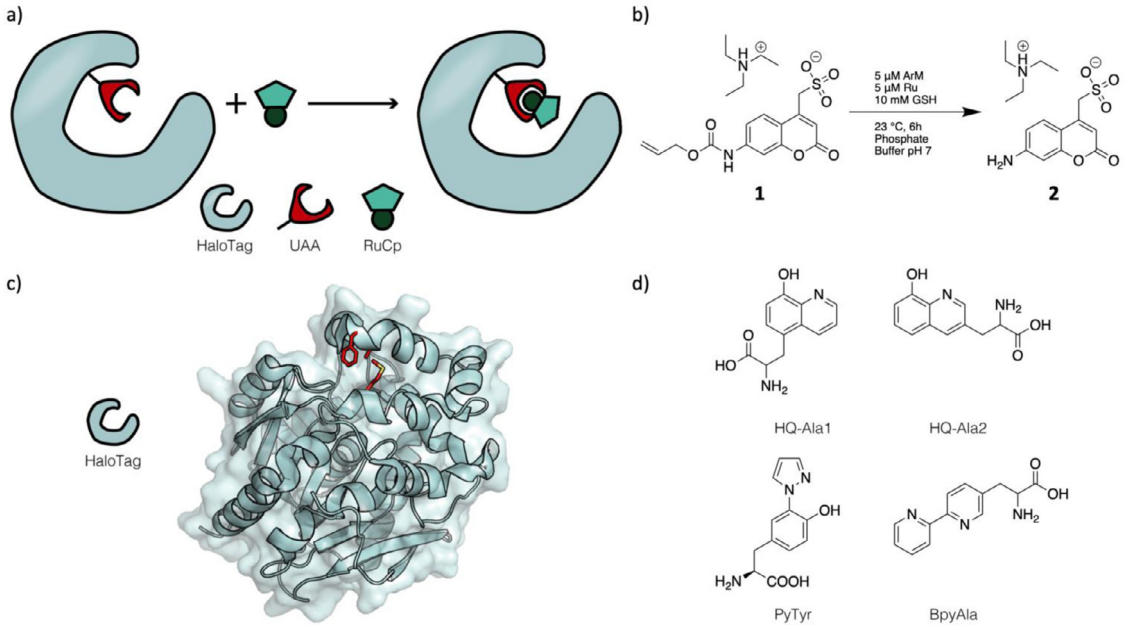

Fig. 1. An artificial deallylase based on the incorporation of a Lewis-basic unnatural amino acid in HaloTag. a) Metal-chelating UAAs are incorporated into HaloTag by amber stop codon suppression to assemble an artificial deallylase after incubation with $[(\eta^5\text{-}C_5H_5)Ru(MeCN)_3]^+$; b) deallylation reaction performed with the ArMs where an O-allyl carbamate-protected coumarin **1** is deprotected to afford the fluorescent product 7-aminocoumarin **2**; c) cartoon representation of a crystal structure of HaloTag (PDB: 5Y2Y [61]) highlighting the three residues selected for UAA incorporation (red); d) structures of the four metal-chelating UAAs used in this project.

2.2. Cloning and expression

To genetically incorporate the UAAs into HaloTag the wildtype HaloTag gene (C-terminally tagged with a factor Xa enzymatic cleavage site followed by a His_6-tag) was modified by site-directed mutagenesis to obtain gene variants with the amber stop codon TAG replacing the codons encoding positions F144, A145 and M175. A pEVOL (Cam^R) plasmid containing the tRNA and tRNA synthetase genes for incorporation of HQ-Ala1 was kindly provided by the Jiangyun Wang group at the Chinese Academy of Sciences (pEVOL-tRNA-UAAtRNAsyn) [51]. The tRNA synthetase sequence was modified by Gibson assembly for the incorporation of HQ-Ala2, Bpy-Ala- and PyTyr. The plasmids containing the modified HaloTag genes were transformed into the competent BL21 (DE3) cells carrying the respective pEVOL-tRNA-UAAtRNAsyn. Expression tests in small culture tubes were carried out in LB media supplemented with kanamycin and chloramphenicol. A preculture was used to inoculate 5 mL cultures which were subsequently incubated at 37 °C for 30 min prior to the addition of the UAA (2 mM for HQ-Ala1, 1 mM for HQ-Ala-2, 1 mM for BpyAla and 0.5 mM for PyTyr). The cultures were incubated further at 37 °C and expression was induced at an OD_{600} of 0.5 by the addition of 1 mM IPTG and 0.2% arabinose.

Medium scale expressions were carried out by inoculating 250 mL autoinduction media containing the respective UAA in a baffled shake flask and incubating the culture for 24 h at 37 °C (Table S3). Please refer to the supplementary information for more detailed information on the described procedures.

2.3. Protein purification and analysis

After pelleting and a freeze-thaw cycle, B-PER cell lysis reagent was added to the cell pellets and incubated for 2 h at room temperature. The cell lysates were cleared by centrifugation (14,000 rpm, 30 min). Ni-NTA resin was equilibrated in Ni-NTA equilibration/binding/wash buffer (20 mM imidazole, 50 mM Tris, 300 mM NaCl, pH 7.4) and subsequently added into PD-10 columns (TELOS) for gravity flow protein purification. The lysates were mixed with 2x Ni-NTA equilibration/binding/wash buffer and loaded onto the column. The unspecifically-bound protein was washed off using ten column volumes of Ni-NTA equilibration/binding/wash buffer. The protein was eluted using Ni-NTA elution buffer (250 mM imidazole, 20 mM Tris, 300 mM NaCl, pH 7.4) and dialyzed into Tris buffer (20 mM Tris, pH 7.4). The solution was concentrated with centrifugal concentrators (Sartorius, 10 K MWCO) to a concentration of 2 mg/mL and flash frozen in liquid nitrogen for storage at – 80 °C. Small-scale purification were purified by a pull-down assay in Eppendorf tubes using the same lysis procedure, resin and buffers. Protein expression was verified by SDS-PAGE with purified protein sample (30 μL) mixed with the sample loading dye (6 μL, 160 mM Tris, 0.04% bromophenol blue, 20% glycerol, 4% SDS). For mass spectrometry analyses, solutions of 0.1 mg/mL protein were prepared in water containing 0.1% formic acid.

2.4. Catalysis

After His_6-tag removal, catalysis was performed in 96-well plates using purified protein (5 μM), $[(\eta^5\text{-}C_5H_5)Ru(MeCN)_3]PF_6$ (5 μM), substrate 1 (1 mM) and GSH (10 mM) in phosphate buffer pH 7 (100 mM, 57.7 mL of 1 M Na_2HPO_4, 42.3 mL 1 M NaH_2PO_4 in water in a total volume of 1 L). Subsequently, GSH and the substrate were added to a total reaction volume of 100 μL. Fluorescence measurements were carried out for 6 h with measurements every 15 min ($\lambda_{excitation}$ = 395 nm and $\lambda_{emission}$ = 460 nm).

2.5. ICP-MS

For ICP-MS measurements, HaloTag-WT and HaloTag-M175-HQ-Ala1 without His_6-tag, BSA, HSA and lysozyme (all 10 μM) were incubated with $[(\eta^5\text{-}C_5H_5)Ru(MeCN)_3]PF_6$ (50 μM) for 45 min. Subsequently, the buffer was exchanged on centrifugal concentrators by five cycles of dilution-concentration with Tris buffer (25 mM). Final protein concentration was adjusted to 1 μM. For the measurements, protein solution (20 μL) was added to ICP-MS buffer (1980 μL, 1% isopropanol, 0.25% ammonia, 20 mg Rhodium

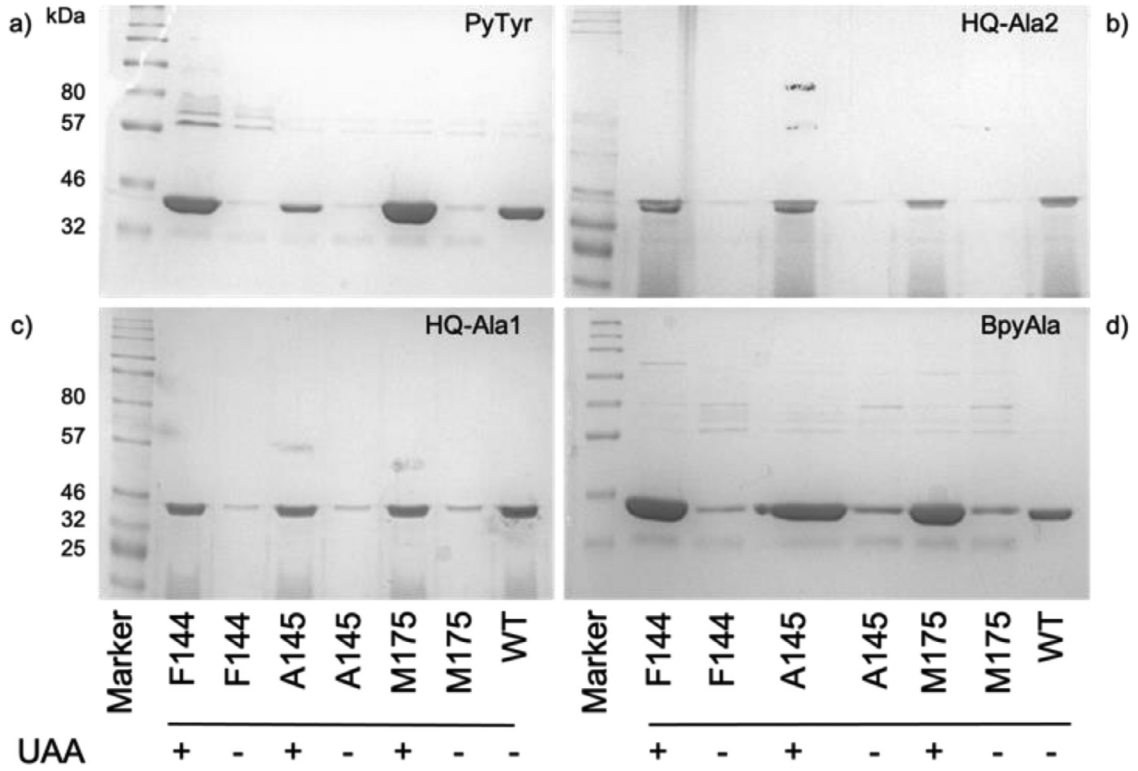

Fig. 2. Incorporation of metal-chelating UAAs into HaloTag at position F144, A145 and M175. Incorporation of a) PyTyr; b) HQ-Ala2; c) HQ-Ala1 and d) BpyAla into HaloTag with (+) or without (-) the addition of the respective UAA.

20 mg Rhenium in 500 mL water). As a calibration, a ruthenium standard solution (1 μM) was prepared.

3. Results

To explore UAA-templated catalysis in HaloTag, four metal-chelating UAAs were selected for the incorporation into HaloTag: HQ-Ala1, HQ-Ala2, PyTyr and BpyAla (Fig. 1d). Within HaloTag, three positions that lie in proximity of the binding-cleft of HaloTag were evaluated for the incorporation of the four UAAs: F144, A145 and M175 (Fig. 1c). For the incorporation of UAAs by amber stop codon suppression, the codons for the selected residues were replaced by a UAG stop codon by site-directed mutagenesis. For each of the four UAAs, small-scale expression tests were carried out to determine the robustness of incorporation (Fig. 2). In each expression test, the protein production was assessed with and without the addition of the respective UAA. Full-length HaloTag was purified by affinity chromatography in the presence of all four UAAs with low background in the absence of the UAA (Fig. 2). These results reveal that each of these UAAs can be readily incorporated at any of these three sites.

To further characterize the incorporation of selected mutants, five variants were expressed in 200 mL cultures and purified with Ni-NTA columns with yields up to 12 mg from a 200 mL culture. Following purification by affinity chromatography, the samples were subjected to mass spectrometry (MS) analysis, thus confirming the incorporation of the UAAs into these mutants (Table 1). Importantly, the MS spectra also confirmed that background expression in the absence of UAA does not lead to the incorporation of alternative amino acids in the presence of the UAA, since the spectra reveal exclusively the UAA-containing protein (Figure S1).

Next, HaloTag with an engineered HQ-Ala1 at either F144, A145 or M175 were selected for medium scale protein expression and purification. The resulting samples were evaluated as host for catalysis. As the in vivo CpRu-catalyzed deallylation is markedly more efficient in the presence of hydroxyquinoline-based bidendate ligands [57], we selected HQ-Ala1 –which is significantly easier to synthesize than HQ-Ala2– as UAA to assemble an artificial deallylase based on the Halotag host protein [58]. Positions F144, A145 and M175 of HaloTag were selected for the introduction of HQ-Ala1 as they lie in the proximity of the hydrophobic HaloTag binding cleft [61]. To assess the catalytic performance, an O-allyl carbamate-protected coumarin **1** was deprotected by the ArMs bearing the Lewis-basic UAA following the addition of $[(\eta^5\text{-}C_5H_5)Ru(MeCN)_3]^+$. The deallylation reaction converts the non-fluorescent substrate **1** to the fluorescent product 7-aminocoumarin **2** which can conveniently be monitored by fluorescence spectroscopy.

Table 1
Mass spectrometry data for the purified HaloTag variants.

HaloTag Variant	Expected Mass (Da)	Measured Mass (Da)
HaloTag-F144-HQ-Ala1	34,367	34,367
HaloTag-A145-HQ-Ala1	34,443	34,443
HaloTag-M175-HQ-Ala1	34,384	34,383
HaloTag-F144-HQ-Ala2	34,367	34,367
HaloTag-M175-HQ-Ala2	34,384	34,383
HaloTag-M175-BpyAla	34,394	34,394

For the catalytic reactions, the HaloTag variants with a factor Xa recognition site between HaloTag and the His_6-tag were expressed and purified using an Ni-NTA resin. Following affinity purification, the His_6-tag was removed by enzymatic cleavage with factor Xa. Complete His_6-tag removal was verified by MS for HaloTag-F144-HQ-Ala1 (Figure S2). Catalysis was carried out upon mixing the protein (5 μM), $[(\eta^5\text{-}C_5H_5)Ru(MeCN)_3]^+$ (5 μM), glutathione (GSH, 10 mM) and substrate **1** in phosphate buffer at pH 7.0. The progress of the reaction was monitored in a Tecan plate

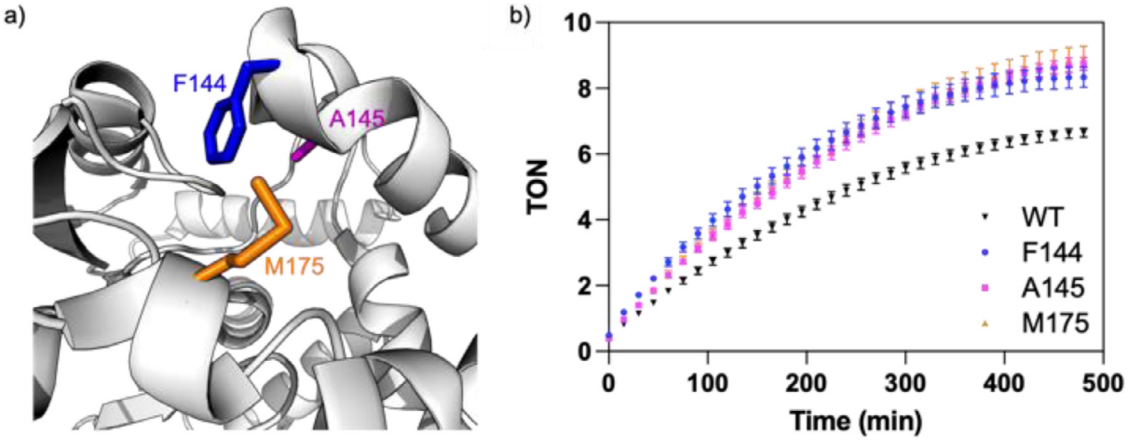

Fig. 3. Deallylation with UAA-HaloTag. a) HaloTag (PDB: 6U32 [62]) with labelled positions F144, A145 and M175 where the HQ-Ala1 was incorporated; b) fluorescence monitoring of the 7-aminocoumarin **2** formation ($\lambda_{excitation}$ = 395 nm and $\lambda_{emission}$ = 460 nm) for HaloTag-WT, HaloTag-F144-HQ-Ala1, HaloTag-A145-HQ-Ala1 and HaloTag-M175-HQ-Ala1.

Table 2
Ruthenium concentrations determined by ICP-MS for different proteins.

Protein[a]	Ru (μM)	Protein (μM)	Molar Ratio of Ru to Protein
HaloTag-WT	0.742 ± 0.026	1.0	0.742 ± 0.026
HaloTag-M175-HQ-Ala1	0.926 ± 0.031	1.0	0.926 ± 0.031
BSA	0.903 ± 0.028	1.0	0.903 ± 0.028
HSA	0.856 ± 0.025	1.0	0.856 ± 0.025
Lysozyme	0.503 ± 0.027	1.0	0.503 ± 0.027

[a] Protein (10 μM) were incubated with 50 μM $[(\eta^5\text{-}C_5H_5)Ru(MeCN)_3]PF6$ for 45 min. Buffer was exchanged by repeated cycles of dilution-concentration with 25 mM Tris buffer and the final protein concentration was adjusted to 1 μM and these samples were analyzed by ICP-MS.

reader with an excitation at 360 nm and an emission at 470 nm, diagnostic for the formation of the uncaged 7-aminocoumarin **2**.

All three UAA-containing HaloTag variants outperform HaloTag-WT with up to 9 turnovers for HaloTag-M175-HQ-Ala1 (Fig. 3). To determine if the UAA indeed binds the CpRu-moiety in the HaloTag variants, the ruthenium content was determined for the best performing ArM as well as the HaloTag-WT (i.e. $[(\eta^5\text{-}C_5H_5)Ru(MeCN)_3]^+$•HaloTag-M175HQ-Ala1 and $[(\eta^5\text{-}C_5H_5)Ru(MeCN)_3]^+$•HaloTag-WT) by ICP-MS. For this purpose, $[(\eta^5\text{-}C_5H_5)Ru(MeCN)_3]^+$ was incubated with HaloTag (10 μM) for 45 min; the buffer was exchanged on a spin concentrator column by five cycles of dilution-concentration with Tris buffer (25 mM). As anticipated, HaloTag-M175-HQ-Ala1 contained more ruthenium than HaloTag-WT. The same procedure was applied to samples of human serum albumin (HSA), bovine serum albumin (BSA) and lysozyme. Ruthenium bound to HaloTag-WT likely corresponds to unspecific binding as the concentrations are similar to those obtained with HSA, BSA and lysozyme (Table 2). Previous studies revealed that Lewis-basic residues including histidine [63–67] and aspartate [68] bind ruthenium ions. Accordingly, we hypothesize that these residues bind to ruthenium ions thus accounting for the [Ru] accumulation and the background catalysis in the presence HaloTag-WT. For comparison, HaloTag-WT contains six surface histidines, seventeen surface aspartates and 20 surface glutamates compared to lysozyme (9 Asp, 8 Glu, 1 His-on surface), HSA (26 Asp, 49 Glu, 9 His-on surface) and BSA (37 Asp, 49 Glu, 11 His-on surface). Unfortunately, attempts to monitor the site-specific coordination of $\{CpRu\}^{2+}$ to the hydroxyquinoline moiety by either UV–Vis or CD-spectroscopy did not reveal any specific spectroscopic signature, that would have enabled the determination of the metal-binding affinity to the HQ-Ala1 (versus the other accessible Lewis-basic residues of either HaloTag-M175-HQ-Ala1 or HaloTag-WT).

4. Conclusion

HaloTag is a promising new scaffold for the assembly of ArMs. Liang et al. recently reported its use as host protein for the assembly of an ArM for olefin metathesis [35]. Herein, we report on the introduction of four metal-chelating UAAs into HaloTag. Each of these UAAs could be incorporated at the three selected HaloTag amino acid positions, in the immediate proximity of the hydrophobic cleft. Upon addition of $[(\eta^5\text{-}C_5H_5)Ru(MeCN)_3]^+$ to three variants containing HQ-Ala1, the resulting ArM performed slightly better than HaloTag-WT for the uncaging of alloc-protected coumarin **1**, to afford the corresponding fluorescent coumarin derivative **2** (Fig. 3). This result highlights the potential for engineering defined transition metal-containing active sites into HaloTag equipped with UAAs. Further studies are currently underway to improve the catalytic performance by directed evolution and cofactor design. To secure the position of the metal cofactor, we envisage adding a haloalkane on the Cp moiety leading to a covalent anchor of the cofactor to the reactive Asp 106 residue of HaloTag. In the current study, only HQ-Ala1 was investigated in catalysis while the other four UAAs were selected to probe their incorporation potential. Further studies are under way to investigate catalysis with the other UAAs. The presented ArM does not yet reach the turnover levels of WT-streptavidin which has been employed as an artificial deallylase yielding up to > 60 TON [69,70]. However, to the best of our knowledge, streptavidin has not been used to create an ArM containing UAAs. We have shown that different UAAs can be readily incorporated into HaloTag. In combination with directed evolution, a UAA-containing HaloTag therefore has the po-

tential to further improve catalysis in various reactions including deallylation.

Declaration of Competing Interest

The authors declare that they have no known competing financial interests or personal relationships that could have appeared to influence the work reported in this paper.

Acknowledgements

We thank the Wang lab for kindly proving the pEVOL plasmid. We are greatful to Christoph Saxer and Peter Neyer for their help and assistance with ICP-MS in the Kantonsspital Aarau. We thank Nico Igareta for measuring MS spectra. ADL thanks Marie Curie (H2020- MSCA-IF-2017), TRW thanks the ERC advanced grant (the DrEAM, grant agreement 694424), the Swiss National Science Foundation (Grant SNF Grant 200020_182046) and the NCCR Molecular Systems Engineering for generous support.

Supplementary materials

Supplementary material associated with this article can be found, in the online version, at doi:10.1016/j.jorganchem.2022.122272.

References

[1] F. Schwizer, Y. Okamoto, T. Heinisch, Y. Gu, M.M. Pellizzoni, V. Lebrun, R. Reuter, V. Köhler, J.C. Lewis, T.R. Ward, Artificial metalloenzymes: reaction scope and optimization strategies, Chem. Rev. 118 (2018) 142–231.
[2] A.G. Jarvis, Designer metalloenzymes for synthetic biology: enzyme hybrids for catalysis, Curr. Opin. Chem. Biol. 58 (2020) 63–71.
[3] W.J. Jeong, J. Yu, W.J. Song, Proteins as diverse, efficient, and evolvable scaffolds for artificial metalloenzymes, Chem. Commun. 56 (2020) 9586–9599.
[4] M. Wittwer, U. Markel, J. Schiffels, J. Okuda, D.F. Sauer, U. Schwaneberg, Engineering and emerging applications of artificial metalloenzymes with whole cells, Nat. Catal. 4 (2021) 814–827.
[5] A.S. Klein, C. Zeymer, Design and engineering of artificial metalloproteins: from de novo metal coordination to catalysis, Protein Eng. Des. Sel. 34 (2021) 1–9.
[6] A.D. Liang, J. Serrano-Plana, R.L. Peterson, T.R. Ward, Artificial metalloenzymes based on the biotin–streptavidin technology: enzymatic cascades and directed evolution, Acc. Chem. Res. 52 (2019) 585–595.
[7] K.R. Miller, S. Biswas, A. Jasniewski, A.H. Follmer, A. Biswas, T. Albert, S. Sabuncu, E.L. Bominaar, M.P. Hendrich, P. Moënne-Loccoz, A.S. Borovik, Artificial metalloproteins with dinuclear iron-hydroxido centers, J. Am. Chem. Soc. 143 (2021) 2384–2393.
[8] R.L. Baughn, Ó. Adalsteinsson, G.M. Whitesides, Conversion of a protein to a homogeneous asymmetric hydrogenation catalyst by site-specific modification with a diphosphinerhodium(I) moiety, J. Am. Chem. Soc. 100 (1978) 306–307.
[9] G. Roelfes, LmrR: a privileged scaffold for artificial metalloenzymes, Acc. Chem. Res. 52 (2019) 545–556.
[10] C. Mayer, C. Dulson, E. Reddem, A.-M.W.H. Thunnissen, G. Roelfes, Directed evolution of a designer enzyme featuring an unnatural catalytic amino acid, Angew. Chemie Int. Ed. 58 (2019) 2083–2087.
[11] K. Oohora, T. Hayashi, Myoglobins engineered with artificial cofactors serve as artificial metalloenzymes and models of natural enzymes, Dalt. Trans. 50 (2021) 1940–1949.
[12] H.M. Key, P. Dydio, D.S. Clark, J.F. Hartwig, Abiological catalysis by artificial haem proteins containing noble metals in place of iron, Nature 534 (2016) 534–537.
[13] M. Pott, T. Hayashi, T. Mori, P.R.E. Mittl, A.P. Green, D. Hilvert, A noncanonical proximal heme ligand affords an efficient peroxidase in a globin fold, J. Am. Chem. Soc. 140 (2018) 1535–1543.
[14] K.D. Miner, A. Mukherjee, Y.G. Gao, E.L. Null, I.D. Petrik, X. Zhao, N. Yeung, H. Robinson, Y. Lu, A designed functional metalloenzyme that reduces O2 to H2O with over one thousand turnovers, Angew. Chemie - Int. Ed. 51 (2012) 5589–5592.
[15] M.R. Duff, J.M. Borreguero, M.J. Cuneo, A. Ramanathan, J. He, G. Kamath, S.C. Chennubhotla, F. Meilleur, E.E. Howell, K.W. Herwig, D.A.A. Myles, P.K. Agarwal, Modulating Enzyme Activity by Altering Protein Dynamics with Solvent, Biochemistry. 57 (2018) 4263–4275.
[16] M. Ohashi, T. Koshiyama, T. Ueno, M. Yanase, H. Fujii, Y. Watanabe, Preparation of artificial metalloenzymes by insertion of chromium (III) Schiff base complexes into apomyoglobin mutants, Angew. Chemie Int. Ed. 42 (2003) 1005–1008.
[17] D.A. Vargas, A. Tinoco, V. Tyagi, R. Fasan, Myoglobin-catalyzed C−H functionalization of unprotected indoles, Angew. Chemie - Int. Ed. 57 (2018) 9911–9915.
[18] F.W. Monnard, E.S. Nogueira, T. Heinisch, T. Schirmer, T.R. Ward, Human carbonic anhydrase II as host protein for the creation of artificial metalloenzymes : the asymmetric transfer hydrogenation of imines, Chem. Sci. 4 (2013) 3269–3274.
[19] P. Dydio, H.M. Key, A. Nazarenko, J.Y.-E. Rha, V. Seyedkazemi, D.S. Clark, J.F. Hartwig, An artificial metalloenzyme with the kinetics of native enzymes, Science 354 (2016) 102–106.
[20] G. Li, Y. Dong, M.T. Reetz, Can machine learning revolutionize directed evolution of selective enzymes? Adv. Synth. Catal. 361 (2019) 2377–2386.
[21] C.G. Acevedo-Rocha, A. Li, L. D'Amore, S. Hoebenreich, J. Sanchis, P. Lubrano, M.P. Ferla, M. Garcia-Borràs, S. Osuna, M.T. Reetz, Pervasive cooperative mutational effects on multiple catalytic enzyme traits emerge via long-range conformational dynamics, Nat. Commun. 12 (2021) 1–13.
[22] O. Shoji, Y. Watanabe, Monooxygenation of nonnative substrates catalyzed by bacterial cytochrome P450s facilitated by decoy molecules, Chem. Lett. 46 (2017) 278–288.
[23] S.N. Natoli, J.F. Hartwig, Noble-metal substitution in hemoproteins: an emerging strategy for abiological catalysis, Acc. Chem. Res. 52 (2019) 326–335.
[24] X. Ren, R. Fasan, Engineered and artificial metalloenzymes for selective C–H functionalization, Curr. Opin. Green Sustain. Chem. 31 (2021) 100494.
[25] M. Planchestainer, N. Segaud, M. Shanmugam, J. McMaster, F. Paradisi, M. Albrecht, Carbene in cupredoxin protein scaffolds: replacement of a histidine ligand in the active site substantially alters copper redox properties, Angew. Chemie - Int. Ed. 57 (2018) 10677–10682.
[26] J.C. Lewis, Beyond the second coordination sphere: engineering dirhodium artificial metalloenzymes to enable protein control of transition metal catalysis, Acc. Chem. Res. 52 (2019) 576–584.
[27] D.F. Sauer, M. Wittwer, U. Markel, A. Minges, M. Spiertz, J. Schiffels, M.D. Davari, G. Groth, J. Okuda, U. Schwaneberg, Chemogenetic engineering of nitrobindin toward an artificial epoxygenase, Catal. Sci. Technol. 11 (2021) 4491–4499.
[28] C. Zhang, P. Srivastava, K. Ellis-Guardiola, J.C. Lewis, Manganese terpyridine artificial metalloenzymes for benzylic oxygenation and olefin epoxidation, Tetrahedron 23 (2014) 4245–4249.
[29] T.C. Chang, K. Vong, T. Yamamoto, K. Tanaka, Prodrug activation by gold artificial metalloenzyme-catalyzed synthesis of phenanthridinium derivatives via hydroamination, Angew. Chemie - Int. Ed. 60 (2021) 12446–12454.
[30] J.H. Mills, W. Sheffler, M.E. Ener, P.J. Almhjell, G. Oberdorfer, J.H. Pereira, F. Parmeggiani, B. Sankaran, P.H. Zwart, D. Baker, Computational design of a homotrimeric metalloprotein with a trisbipyridyl core, Proc. Natl. Acad. Sci. 113 (2016) 15012–15017.
[31] B. Kuhlman, G. Dantas, G.C. Ireton, G. Varani, B.L. Stoddard, D. Baker, Design of a novel globular protein fold with atomic-level accuracy, Science 302 (2003) 1364–1369.
[32] W.J. Song, F.A. Tezcan, A designed supramolecular protein assembly with in vivo enzymatic activity, Science 346 (2014) 1525–1528.
[33] T.B.J. Pinter, K.J. Koebke, V.L. Pecoraro, Catalysis and electron transfer in de novo designed helical scaffolds, Angew. Chemie - Int. Ed. 59 (2020) 7678–7699.
[34] E.N. Mirts, I.D. Petrik, P. Hosseinzadeh, M.J. Nilges, Y. Lu, A designed heme-[4Fe-4S] metalloenzyme catalyzes sulfite reduction like the native enzyme, Science 361 (2018) 1098–1101.
[35] S. Fischer, T.R. Ward, A.D. Liang, Engineering a metathesis-catalyzing artificial metalloenzyme based on HaloTag, ACS Catal 11 (2021) 6343–6347.
[36] G.V. Los, L.P. Encell, M.G. Mcdougall, D.D. Hartzell, N. Karassina, C. Zimprich, M.G. Wood, R. Learish, R. Friedmann Ohana, M. Urh, D. Simpson, J. Mendez, K. Zimmerman, P. Otto, G. Vidugiris, J. Zhu, A. Darzins, D.H. Klaubert, R.F. Bulleit, K.V. Wood, HaloTag: a novel protein labeling technology for cell imaging and protein analysis, ACS Chem. Biol. 3 (2008) 373–382.
[37] L. Wang, A. Brock, B. Herberich, P.G. Schultz, Expanding the genetic code of Escherichia coli, Science 292 (2001) 498–500.
[38] I. Drienovská, G. Roelfes, Expanding the enzyme universe with genetically encoded unnatural amino acids, Nat. Catal. 3 (2020) 193–202.
[39] W. Liu, A. Brock, S. Chen, S. Chen, P.G. Schultz, Genetic incorporation of unnatural amino acids into proteins in mammalian cells, Nat. Methods. 4 (2007) 239–244.
[40] S. Greiss, J.W. Chin, Expanding the genetic code of an animal, J. Am. Chem. Soc. 133 (2011) 14196–14199.
[41] P.J. Almhjell, J.H. Mills, Metal-chelating non-canonical amino acids in metalloprotein engineering and design, Curr. Opin. Struct. Biol. 51 (2018) 170–176.
[42] C. Hu, S.I. Chan, E.B. Sawyer, Y. Yu, J. Wang, Metalloprotein design using genetic code expansion, Chem. Soc. Rev. 43 (2014) 6498–6510.
[43] H.S. Lee, G. Spraggon, P.G. Schultz, F. Wang, Genetic incorporation of a metal-ion chelating amino acid into proteins as a biophysical probe, J. Am. Chem. Soc. 131 (2009) 2481–2483.
[44] Y. Yu, C. Hu, L. Xia, J. Wang, Artificial metalloenzyme design with unnatural amino acids and non-native cofactors, ACS Catal 8 (2018) 1851–1863.
[45] S.J. Opella, S. Berkamp, S.H. Park, V.S. Wang, A.A. De Angelis, J. Radoicic, Paramagnetic relaxation enhancement of membrane proteins by incorporation of the metal-chelating unnatural amino acid 2-amino-3-(8-hydroxyquinolin-3-yl)propanoic acid (HQA), J. Biomol. NMR. 61 (2014) 185–196.
[46] X. Liu, Y. Yu, C. Hu, W. Zhang, Y. Lu, J. Wang, Significant increase of oxidase activity through the genetic incorporation of a tyrosine-histidine cross-link in a

myoglobin model of heme-copper oxidase, Angew. Chemie - Int. Ed. 51 (2012) 4312–4316.
[47] X. Liu, J. Li, J. Dong, C. Hu, W. Gong, J. Wang, Genetic incorporation of a metal-chelating amino acid as a probe for protein electron transfer, Angew. Chemie Int. Ed. 51 (2012) 10261–10265.
[48] M. Bersellini, G. Roelfes, Multidrug resistance regulators (MDRs) as scaffolds for the design of artificial metalloenzymes, Org. Biomol. Chem. 15 (2017) 3069–3073.
[49] J.H. Mills, S.D. Khare, J.M. Bolduc, F. Forouhar, V.K. Mulligan, S. Lew, J. Seetharaman, L. Tong, B.L. Stoddard, D. Baker, Computational design of an unnatural amino acid dependent metalloprotein with atomic level accuracy, J. Am. Chem. Soc. 135 (2013) 13393–13399.
[50] G.E. Merz, P.P. Borbat, A.R. Muok, M. Srivastava, D.N. Bunck, J.H. Freed, B.R. Crane, Site-specific incorporation of a Cu2+ spin label into proteins for measuring distances by pulsed dipolar electron spin resonance spectroscopy, J. Phys. Chem. B. 122 (2018) 9443–9451.
[51] X. Liu, J. Li, C. Hu, Q. Zhou, W. Zhang, M. Hu, J. Zhou, J. Wang, Significant expansion of the fluorescent protein chromophore through the genetic incorporation of a metal-chelating unnatural amino acid, Angew. Chemie - Int. Ed. 52 (2013) 4805–4809.
[52] I. Drienovská, A. Rioz-Martínez, A. Draksharapu, G. Roelfes, Novel artificial metalloenzymes by in vivo incorporation of metal-binding unnatural amino acids, Chem. Sci. 6 (2015) 770–776.
[53] T. Hayashi, D. Hilvert, A.P. Green, Engineered metalloenzymes with non-canonical coordination environments, Chem. - A Eur. J. 24 (2018) 11821–11830.
[54] E.N. Mirts, A. Bhagi-Damodaran, Y. Lu, Understanding and modulating metalloenzymes with unnatural amino acids, non-native metal ions, and non-native metallocofactors, Acc. Chem. Res. 52 (2019) 935–944.
[55] I. Drienovská, R.A. Scheele, C. Gutiérrez de Souza, G. Roelfes, A hydroxyquinoline-based unnatural amino acid for the design of novel artificial metalloenzymes, ChemBioChem 21 (2020) 3077–3081.
[56] C. Streu, E. Meggers, Ruthenium-induced allylcarbamate cleavage in living cells, Angew. Chemie - Int. Ed. 45 (2006) 5645–5648.
[57] T. Völker, E. Meggers, Chemical activation in blood serum and human cell culture: improved ruthenium complex for catalytic uncaging of alloc-protected amines, ChemBioChem 18 (2017) 1083–1086.
[58] T. Völker, F. Dempwolff, P.L. Graumann, E. Meggers, Progress towards bioorthogonal catalysis with organometallic compounds, Angew. Chem. Int. Ed. Engl. 53 (2014) 10536–10540.
[59] M. Tomás-Gamasa, M. Martínez-Calvo, J.R. Couceiro, J.L. Mascarenãs, Transition metal catalysis in the mitochondria of living cells, Nat. Commun. 7 (2016).
[60] Z. Zhou, G. Roelfes, Synergistic catalysis in an artificial enzyme by simultaneous action of two abiological catalytic sites, Nat. Catal. 3 (2020) 289–294.
[61] M.G. Kang, H. Lee, B.H. Kim, Y. Dunbayev, J.K. Seo, C. Lee, H.W. Rhee, Structure-guided synthesis of a protein-based fluorescent sensor for alkyl halides, Chem. Commun. 53 (2017) 9226–9229.
[62] C. Deo, A.S. Abdelfattah, H.K. Bhargava, A.J. Berro, N. Falco, H. Farrants, B. Moeyaert, M. Chupanova, L.D. Lavis, E.R. Schreiter, The HaloTag as a general scaffold for far-red tunable chemigenetic indicators, Nat. Chem. Biol. 17 (2021) 718–723.
[63] D. Stanic-Vucinic, S. Nikolic, K. Vlajic, M. Radomirovic, J. Mihailovic, T. Cirkovic Velickovic, S. Grguric-Sipka, The interactions of the ruthenium(II)-cymene complexes with lysozyme and cytochrome c, J. Biol. Inorg. Chem. 25 (2020) 253–265.
[64] I.W. McNae, K. Fishburne, A. Habtemariam, T.M. Hunter, M. Melchart, F. Wang, M.D. Walkinshaw, P.J. Sadler, Half-sandwich arene ruthenium(II)–enzyme complex, Chem. Commun. (2004) 1786–1787.
[65] F. Lupi, T. Marzo, G. D'Adamio, S. Cretella, F. Cardona, L. Messori, A. Goti, Diruthenium diacetate catalysed aerobic oxidation of hydroxylamines and improved chemoselectivity by immobilisation to lysozyme, ChemCatChem 9 (2017) 4225–4230.
[66] A. Casini, G. Mastrobuoni, W.H. Ang, C. Gabbiani, G. Pieraccini, G. Moneti, P.J. Dyson, L. Messori, ESI-MS characterisation of protein adducts of anticancer ruthenium(II)-arene PTA (RAPTA) complexes, ChemMedChem 2 (2007) 631–635.
[67] D. Valensin, P. Anzini, E. Gaggelli, N. Gaggelli, G. Tamasi, R. Cini, C. Gabbiani, E. Michelucci, L. Messori, H. Kozlowski, G. Valensin, Fac-{Ru(CO)3}2+ selectively targets the histidine residues of the β-amyloid peptide 1-28. Implications for new alzheimer's disease treatments based on ruthenium complexes, Inorg. Chem. 49 (2010) 4720–4722.
[68] L. Messori, A. Merlino, Ruthenium metalation of proteins: the X-ray structure of the complex formed between NAMI-A and hen egg white lysozyme, Dalt. Trans. 43 (2014) 6128–6131.
[69] E. Boros, F. Sebák, D. Héja, D. Szakács, K. Zboray, G. Schlosser, A. Micsonai, J. Kardos, A. Bodor, G. Pál, Directed evolution of canonical loops and their swapping between unrelated serine proteinase inhibitors disprove the inter-scaffolding additivity model, J. Mol. Biol. 431 (2019) 557–575.
[70] A. Baiyoumy, J. Vallapurackal, F. Schwizer, T. Heinisch, T. Kardashliev, M. Held, S. Panke, T.R. Ward, Directed evolution of a surface-displayed artificial allylic deallylase relying on a GFP reporter protein, ACS Catal 11 (2021) 10705–10712.